Electronic Supplementary Material (ESI) for RSC Advances.

Electronic Supporting Information

Three-Dimensional Plasmonic Hydrogel Architecture: Facile Synthesis and Its Macro Scale Effective Space

Lei Ouyang, Lihua Zhu*, Jizhou Jiang, Wei Xie, Heqing Tang*

Table of Contents

Difference between “active depth” and “effective depth”

To make a distinction between conventional “active depth” and “effective depth” we proposed, here we made an illustration.

It is generally accepted that confocal Raman microscope possesses a sensitive depth resolution, theoretically only the signal which come to the confocal plane would be collected by detector. But as a matter of fact, due to the limitation of instrument, not only the signal at the confocal plane but also in a circular truncated cone near it would be effective for SERS intensity. Experimentally, a single crystal silicon wafer can be used to provide the confocal depth profile by depth scanning. The depth profile of the Raman intensity was distributed in a nearly gaussian fashion. The active depth “h” was defined as the half band width of the depth profile, which represented that the contribution from depth within h would be effective for detector. The h value depends on the pinhole size and the objective lens of the Raman instrument. This value can be considered as the key parameter of the confocal characteristic.[S2]

For a solution or common used low dimensional substrate, due to the instrument’s confocal property, the contribution from space that out of “active depth” would be negligible. But in our case, the Ag NPs were distributed uniformly within the transparent hydrogel, all Ag NPs within illuminated volume of gel gave out SERS signal. And the NPs gave out multiple reflections and refractions within the illuminated volume would surely contribute to more signal to get to the confocal plane that would be collected by the detector. To clearly exhibit the 3D volume that effectively contributed to the collected signal, we defined the “effective depth”. Not like the “active depth”, it is not the property of the instrument, but represented the substrate’s ability of making use of 3D volume to SERS intensity. The contribution effect from effective space could be monitored by the depth scanning and slice observation (The results could be found in Fig. 6 and Fig. 7. For the depth profile of our substrate, different from the gaussian distribution of signal intensity of a single crystal silicon wafer, a trend of increasing initially, passing a maximum and decreased then with increasing the z depth was obtained. This clearly showed the contribution from space out of confocal plane. The depth from the surface of the substrate to the depth which gave out strongest intensity was defined as the "effective depth" (as shown in Fig. 6e).

EDX spectrum

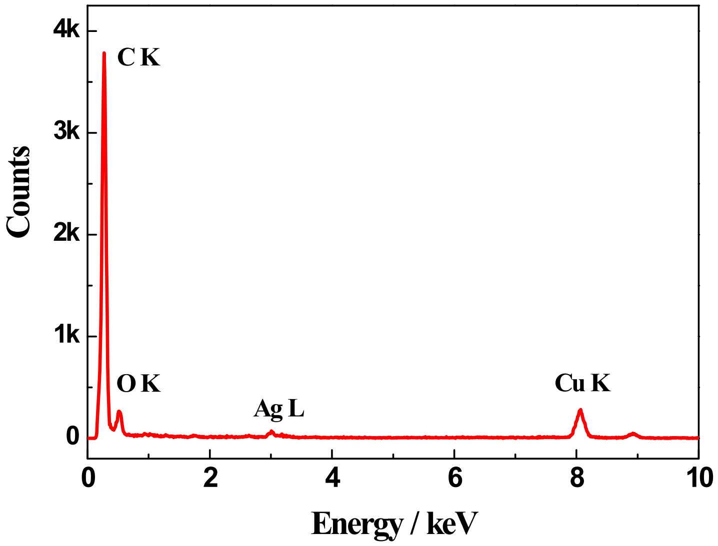

Fig. S1 EDX spectrum of Ag NPs recorded in PVA-1Ag.

Depth scanning for 4-ATP

Fig. S2 Raman depth-scanning images on 8 μM 4-ATP-captured PVA-nAg (at 1075 cm^{-1}). The point-to-point scanning distances in the x and z direction were both 5 μm. The substrates: (a) PVA-1Ag, (b) PVA-1.5Ag, (c) PVA-2Ag, (d) PVA-3Ag, and (e) PVA-5Ag. (f) Effects of the used $AgNO_3$ concentration (the number and size of Ag NPs) on effective depth (H) of PVA-nAg by using the probes of CV (red line) and 4-ATP (blue line).

Illustration of different detect modes

Fig. S3 Illustration of the contribution to SERS from the confocal plane of illuminated PVA-Ag substrate by using (a) depth scanning mode and (b) slice observation mode. The parameters h and d represent the scanning depth and the slice thickness, respectively.

Analyte detection

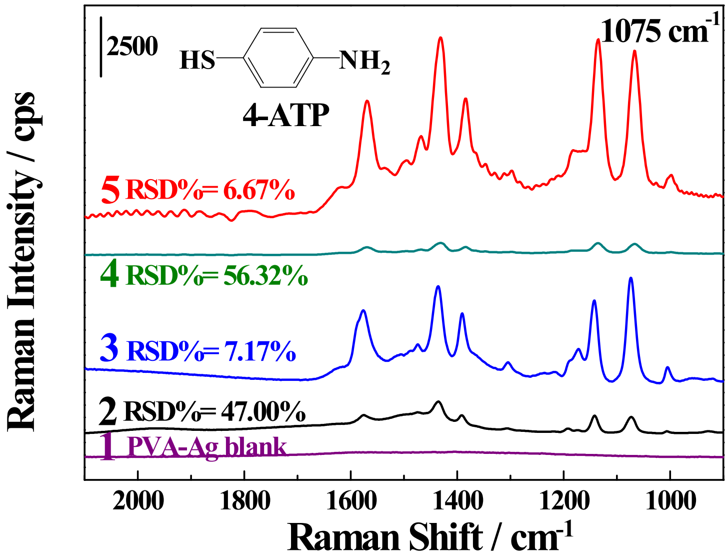

Fig. S4 (1) Background SERS spectra of PVA-2Ag with confocal Raman instrument (780 nm laser, 10mW, 3s×10 times); (2-5) SERS spectra of 8.0 μM 4-ATP with different instruments and substrates; (2）citrate-Ag sol with confocal Raman instrument (780 nm laser, 10mW, 3s×10 times)；(3）PVA-2Ag with confocal Raman instrument(780 nm laser, 10mW, 3s×10 times)； (4) citrate-Ag sol with potable Raman instrument (785 nm laser, 100mW, 3s×10 times); (5) PVA-2Ag with potable Raman instrument (785 nm laser, 100mW, 3s×10 times). The RSD values of the SERS intensity at 1075 cm^{-1} were shown in the figure, and the intensity recording was conducted at 20 spots randomly chosen for each RSD evaluation.

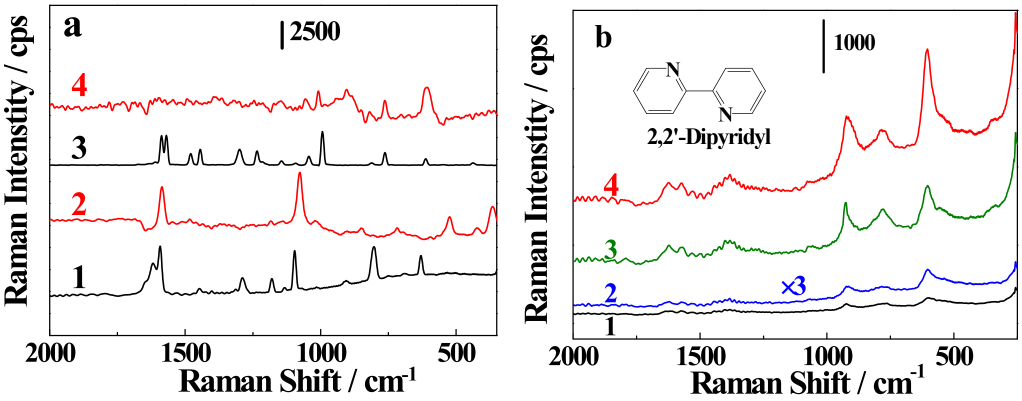

Fig. S5 (a) Raman and SERS spectra of two pollutants. (1) Raman spectrum of 4-MBA powder; (2) SERS spectrum of 1.2×10^{-7} M 4-MBA on PVA-2Ag substrate; (3) Raman spectrum of 2,2'-dipyridyl powder; (4) SERS spectrum of 6.5×10^{-7} M 2,2'-dipyridyl on PVA-2Ag substrate. The SERS spectrum with PVA-2Ag corresponded to the Raman spectrum of related powders. (b) Detection of 2,2'-dipyridyl by using a portable Raman instrument. (1) 6.4×10^{-6} M on citrate-Ag sol; (2) 6.4×10^{-9}, (3) 6.4×10^{-7} and (4) 6.4×10^{-6} M on PVA-2Ag. The detection limit of 2,2'-dipyridyl was 6.4 nM.